Biology of Reproduction, 2019, 101(2), 466–477
doi:10.1093/biolre/ioz107
Research Article
Advance Access Publication Date: 14 June 2019

OXFORD

Research Article

Recruitment of monocytes and mature macrophages in mouse pubic symphysis relaxation during pregnancy and postpartum recovery†

Bianca G. Castelucci, Silvio R. Consonni, Viviane S. Rosa and Paulo P. Joazeiro*

Department of Biochemistry and Tissue Biology, Institute of Biology, State University of Campinas (UNICAMP), Campinas, Brazil

***Correspondence:** Department of Biochemistry and Tissue Biology, State University of Campinas, CP 6109, Zip Code 13083-970, Campinas, SP, Brazil. Phone: +55-19-3521-6248. E-mail: pjoaz@unicamp.br

†**Grant support:** This work was supported by FAPESP (2012/25038-8, 2015/23616-2) and CNPq (140714/2016-2. 302208/2017-8). BGC and SRC contribute equally to this work.
Conference presentation: Presented in part at the XVII Meeting of the Brazilian Society for Cell Biology, 3–6 September 2014, Foz do Iguaçu, Brazil, and at the Workshop on Recent Advances and Applications in Confocal and Widefield Microscopy, 6–8 August 2014, Campinas, Brazil.
Edited by Dr. Lane K. Christenson, PhD, University of Kansas Medical Center

Received 7 February 2019; Revised 3 May 2019; Accepted 13 June 2019

Abstract

Appropriate remodeling of the female lower reproductive tract and pelvic floor is essential during normal mammalian pregnancy, labor, and postpartum recovery. During mouse pregnancy, in addition to reproductive tract modifications, the pubic symphysis (PS) is remodeled into a soft interpubic ligament (IpL) to provide safe delivery of the offspring and fast postpartum recovery. Although temporal changes in the phenotypes of myeloid cells, such as mononuclear phagocytes, are crucial to remodeling the lower reproductive tract organs in preparation for a safe delivery, little is known about the involvement of recruited monocytes or macrophages in mouse PS remodeling. We used combined light microscopy, electron microscopy, and qPCR analysis to investigate the profile of recruited monocytes and macrophage polarization markers in C57Bl6 mouse interpubic tissues during pregnancy (D12, D18, and D19) and early days postpartum (1 dpp and 3 dpp) to better identify their presence in proper remodeling of the mouse PS. Our morphological data show that the number of recruited monocytes is increased in interpubic tissues and that recruited monocytes differentiate into proinflammatory or anti-inflammatory macrophage phenotypes from D18 to 3 dpp, which may contribute to dynamic changes in the gene expression of specific inflammatory mediators involved in interpubic tissue remodeling at these time points. Therefore, our morphological and quantitative gene expression data suggest that both differentiated macrophages from recruited monocytes and polarized macrophages may collaborate for IpL relaxation at labor and the appropriate repair of the PS after the first pregnancy.

Summary Sentence

Recruited monocytes and mature macrophages are present in the mouse pubic symphysis and may contribute to mouse pubic symphysis relaxation during late pregnancy and postpartum recovery.

Key words: pubic symphysis, recruited macrophage, tissue remodeling, mouse, pregnancy.

Introduction

In mammals, the remodeling of connective tissue preceding the onset of labor is a hallmark of major histoarchitectural adaptations that occur in the female lower reproductive tract and the musculoskeletal elements surrounding it to facilitate successful parturition [1–4]. These modifications in the uterus, cervix, vagina, and structures that provide tensile strength to the female pelvic floor, such as the endopelvic fascia and parametrial adipose tissue, have demonstrated that the extracellular matrix (ECM) content and cells are drastically altered preceding the onset of labor only to return to nonpregnant levels after postpartum involution [2, 4–7]. Aberrant modifications in mouse ECM molecules in the low reproductive tract or pelvic floor alter the tissue biomechanical behavior of the pelvic organ support during pregnancy, leading to the development of pelvic organ prolapse, an injury related to pregnancy, age, hormonal effects, and vaginal delivery [8–12].

Together with remodeling of the female lower reproductive tract organs and all the pelvic floor tissue, it is well established that mouse pubic symphysis (PS) fibrocartilaginous tissue is remodeled during pregnancy, resulting in pubic bone separation for labor and PS postpartum recovery after the end of the first pregnancy [13–15]. The remodeling of the mouse PS is a finely tuned, hormonally regulated process that involves cartilage and pubic bone reabsorption [13, 16–18] and the formation of a flexible interpubic ligament (IpL) [1, 14, 19, 20] that, under the influence of matrix metalloproteases (MMPs) [21, 22], hyaluronidases [23], and nitric oxide (NO) [24], goes through modifications in ECM composition at the end of pregnancy that result in its relaxation preceding labor. Right after delivery, a fast recovery process takes place to assure reproductive tract homeostasis. At that point, repacking of the IpL collagenous network occurs with its simultaneous reabsorption [25, 26]. Proteinase expression and activity levels progressively decrease to nonpregnant levels after 3 dpp, hyaline cartilage is restored after 10 dpp, and a non-pregnant PS histoarchitecture is re-established after 40 dpp [16, 21, 23, 26, 27].

Along with remodeling of the female lower reproductive tract and pelvic floor connective tissue, temporal changes in the myeloid cells reveal dynamic functions that are crucial to the success of parturition and fast tissue recovery postpartum [28–30]. Among the myeloid cells, macrophage recruitment, traffic, activity, and polarization in both the proinflammatory (M1) and anti-inflammatory (M2) phenotypes are involved in a wide range of gestational processes such as implantation, prevention of the rejection of the fetus, the initiation of labor, and postpartum reproductive tract remodeling [5, 28, 31–36]. Moreover, the depletion of macrophages may interfere with the ripening process and account for delayed parturition [37] and disturbing the physiological system of senescent cell clearance in the postpartum uterus [32], which may be involved in successful postpartum uterine recovery to prepare for the next pregnancy.

Although the beginning of mouse PS remodeling takes place around D14 with pubic bone resorption, as indicated by the presence of many myeloid cells identified as small osteoclasts in the periosteum [13], until now, little was known about the participation of macrophages in mouse fibrocartilaginous interpubic tissue remodeling that were, to our knowledge, described in a pioneering ultrastructural study only as having a "peculiar cell-type" [38]. Later, high levels of mononuclear infiltration were recorded 1 day after guinea pig parturition, without phenotypic characterization [29]. Despite these findings in guinea pig IpL and elevated NO and MMP levels [22, 24] and ECM turnover at labor [16, 23, 26] during mouse PS remodeling demonstrated by molecular assays, there are no reports of agents other than fibroblast-like cells that are capable of triggering the production of these factors during mouse PS remodeling [21, 22, 24]. Therefore, we decided to investigate whether macrophages are part of the IpL cellular milieu at relaxation before birth and during postpartum repair of the interpubic tissues.

To better define the involvement of recruited monocytes and differentiated macrophages during mouse interpubic tissue remodeling at the end of pregnancy and during postpartum recovery, we used light microscopy, electron microscopy, and qPCR analysis to investigate the profile of recruited monocytes and polarized macrophage markers in C57Bl6 mouse interpubic tissues during pregnancy (D12, D18, and D19) and during postpartum recovery (1 dpp and 3 dpp). Morphological analysis identified the presence of both recruited monocytes and macrophages during mouse PS remodeling during late pregnancy and postpartum recovery. We also provide evidence that cells with phenotypes similar to M1 and M2 macrophages are both present in the IpL from D19 to 3 dpp when quantitative gene expression of inflammatory mediators undergoes dynamic changes in gene expression levels. Therefore, these results suggest that these myeloid cell types may collaborate for successful labor and the fast recovery of the postpartum PS.

Materials and methods

Animals

Virgin female C57BL/6/JUnib mice (3 months old) were obtained from the Multidisciplinary Center for Biological Investigation on Laboratory Animal Science at State University of Campinas (UNICAMP). Mating and vaginal plug observation at day 1 of pregnancy (D1) were performed as described by Castelucci and coworkers [16]. PS or IpL samples were obtained on the following days of pregnancy: D12, D18, D19, 1 dpp, and 3 dpp. As a control tissue for immunofluorescent assays, the mouse cervix was obtained at 3 dpp. Three animals per group were used to obtain the interpubic tissues for morphological and immunofluorescence analyses, and three (D18, D19, and 1 dpp) or six (D12 and 3 dpp) animals were used for real-time PCR analysis. In total, 81 animals were used for the experimental analyses. The animal experiments were conducted in accordance with the Guide for the Care and Use of Laboratory Animals issued by the National Institutes of Health (Bethesda, MD). All protocols using mice were approved by the Institutional Committee for Ethics in Animal Research (Comissão de Ética no Uso de Animais-CEUA/IB/UNICAMP, protocols 2995–1 and 3789–1).

Histology

Pubic symphyses or interpubic ligaments were removed from three mice on each day of study (D12, D18, D19, 1 dpp, and 3 dpp); the samples were fixed, processed, embedded in Historesin (Leica Microsystems, Heidelberg, Germany), and sectioned transversely (anteroposterior direction) at a width of 3 μm. The sections were mounted on slides and stained with Giemsa (Sigma) according to Consonni and coworkers [26] or hematoxylin-phloxine B (Sigma) according to Bennett and coworkers [39]. After staining, samples were examined and imaged using a Nikon Eclipse E800 light microscope (Nikon Corporation, Tokyo, Japan).

Transmission electron microscopy

Small samples of the interpubic tissues from three animals per day of study (D12, D18, D19, 1 dpp, and 3 dpp) were fixed in 2.5% glutaraldehyde (Electron Microscope Sciences, Hatfield, PA) in 0.1 M cacodylate buffer containing 0.3% tannic acid for 4 h at 4°C. Tissues were then postfixed with 1% osmium in 0.1 M cacodylate buffer for 1 h, dehydrated through a graded series of acetone, and embedded in Epon (Embed 812; Electron Microscopy Sciences, Hatfield, PA). Ultrathin sections were stained with uranyl acetate and lead citrate for posterior examination with a Zeiss Leo 906 electron microscope (Electron Microscopy Laboratory, IB, UNICAMP).

Scanning electron microscopy

Interpubic tissues from three animals per day of study (D12, D18, D19, 1 dpp, and 3 dpp) were fixed in 2.5% glutaraldehyde in a cacodylate 0.1 M solution with 4% paraformaldehyde (pH 7.4) and processed according to Joazeiro and coworkers [40]. Samples were dried to critical point using liquid CO_2 in a critical point dryer (Balzers CPD 030; Bal-Tec AG, Foehrenweg, Liechtenstein). Finally, samples were mounted on metal stubs with double-sided adhesive tape and coated with gold using a sputter coater (Balzers SCD 050). Observations of the transverse plane through the PS or IpL region were made by scanning electron microscope (SEM; FEI Quanta 650 FEG (FEI Company, Hillsboro, OR)) at an accelerating voltage of 20 kV (Electron Microscopy Laboratory, Brazilian Nanotechnology National Laboratory-LNNano, CNPEM).

Immunofluorescence

The locations of neutrophil 7/4 Ly-6B.2 alloantigen (Neu 7/4) and EGF-like module-containing mucin-like hormone receptor-like 1 (F4/80)-positive cells as well as cells double positive for F4/80 and CD40 or transferrin receptor (TfR) were determined by immunofluorescence assays. Immunolabeling was performed in transverse cryosections (8 μm) of three mouse interpubic tissues at D12, D18, D19, 1 dpp, and 3 dpp and three 3 dpp mouse cervices frozen in n-hexane with liquid nitrogen sectioned in the anteroposterior direction. Cervical sections were defined as slices containing a central portion of the cervix surrounded by uterine horns.

Immunostaining reactions were performed according to Consonni and coworkers [20] using Neu 7/4 (1:300/MCA771GA, Serotec, Raleigh, NC) or F4/80 (1:300/T-2028.0100, BACEM Biosciences, Inc., King of Prussia, PA) antibodies for single labeling and combinations of F4/80 (1:200) and CD40 polyclonal antibody (1:300/ab13545, Abcam plc, Abcam, Cambridge, MA) or TfR polyclonal antibody (1:300/ab84036, Abcam plc, Abcam) for double labeling. Primary antibody incubations were followed by incubation with fluorophore-conjugated (1:500/Alexa Fluor 488 or 1:500/Alexa Fluor 568) secondary antibodies (Abcam), and nuclei were stained with DAPI for 5 min (sc-3598, Santa Cruz). The sections were mounted with Vectashield Mounting Medium (Vector Labs, Burlingame, CA) and visualized with a Leica DM5500B (Laboratory of Nerve Regeneration, UNICAMP), Leica TCS SP8 (Brazilian Biosciences National Laboratory -LNBio, CNPEM), or Zeiss LSM 780-NLO microscope (National Institute of Science and Technology on Photonics Applied to Cell Biology-INFABIC, UNICAMP) using the ×20 and ×40 objectives.

Quantitative real-time PCR

Gene expression levels of the macrophage marker F4/80, the migratory monocyte marker CC chemokine receptor type 2 (CCR2), and markers of M1 and M2 macrophages were analyzed in interpubic tissues from D12 to 3 dpp. Three (D18, D19, and 1 dpp) or six (D12 and 3 dpp) animals were used to obtain 200 ng of total RNA for each day of study, and all reactions were performed in triplicate on the same plate. Total RNA from mice was extracted from frozen interpubic tissues from D12 to 3 dpp using TRIzol Reagent (Invitrogen Life Technologies), and cDNA was synthesized using a RevertAid H Minus First Strand cDNA Synthesis Kit (Fermentas, MD). Both procedures were carried out according to the manufacturer's recommendations. Real-time PCR was performed using SYBR Green (Applied Biosystems, Foster City, CA) in an Applied Biosystems 7300 system (LNBio, CNPEM). Each gene was normalized to the expression of the housekeeping gene *36b4*. To quantify and determine the fold increase in gene expression, the 2-ΔΔCt mathematical model was utilized, and the results were normalized to those of experiments with the D12 group as performed by Consonni and coworkers [20]. The primers for *36b4*, CC chemokine receptor type 2 (*Ccr2*), *F4/80*, M1 related genes [interleukin 1a *(Il1a)* and tumor necrosis factor alpha (*Tnf-alpha)*], and M2 related genes [arginase (*Arg1*), interleukin 10 (*Il10*), and transforming growth factor beta (*Tgf-beta*)] were purchased from Applied Biosystems (see Supplemental Table S1 for primer sequences).

Statistical analysis

For Neu 7/4 and F4/80-positive quantification in the IpL, cells were counted with NIH ImageJ and normalized to cell nuclei according to Heuerman and coworkers [41]. Therefore, five images of the interpubic tissues of three animals from D18 to 3 dpp were used. For each image, nuclei were counted by the ImageJ particle analysis tool to obtain the total number of cells, and Neu 7/4- and F4/80-positive cells were manually counted utilizing the ImageJ Cell counting plugin [42]. The variance in the percentages of positive cells for each marker during interpubic tissue remodeling was analyzed by performing one-way ANOVA (significance = $P < 0.05$; GraphPad Prism 5.0, GraphPad Software, Inc., CA). The relative gene expression analysis was performed based on the methods of Conover and Iman [43] and Montgomery [44] using rank data classification and semiparametric analysis (one-way ANOVA followed by the Tukey test or two-way ANOVA followed by the Bonferroni test) with $P < 0.05$ indicating significance performed by GraphPad Prism 5.0 (GraphPad Software, Inc.). All data are presented in graphs as the mean value ± standard error (SE).

Results

Mononuclear phagocytes in pubic symphysis remodeling during the end of pregnancy and early postpartum recovery

To identify mononuclear phagocytic-like cells in mouse interpubic tissues from D12 to 3 dpp, we examined PS and IpL transverse slices

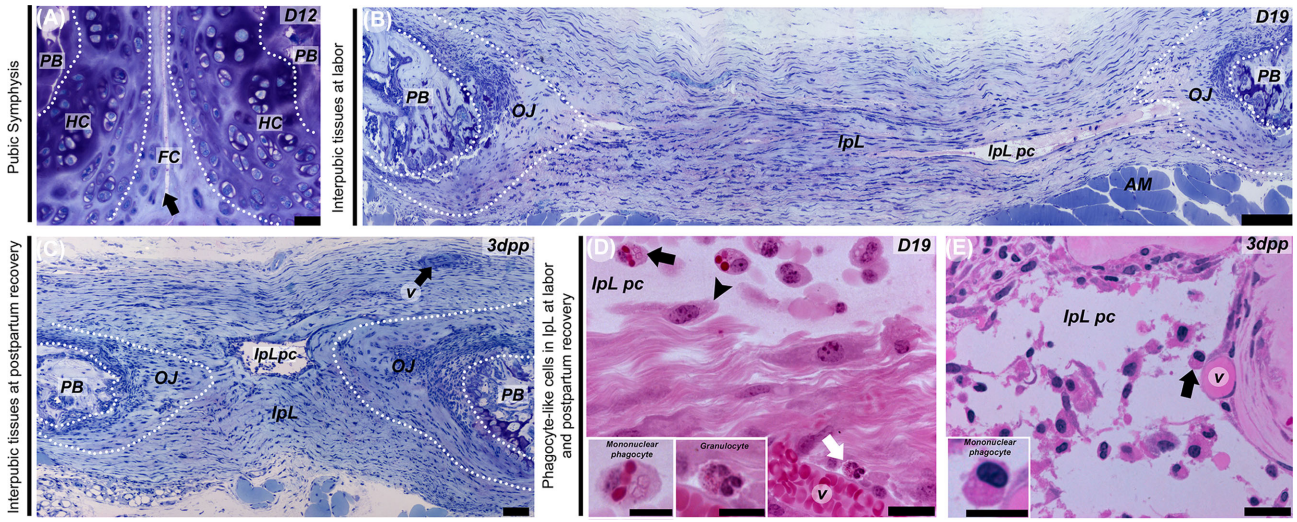

Figure 1. Light micrographs of resin-embedded tissue sections of the PS at D12 (A) and the IpL at D19 (B and D) and 3 dpp (C and E). (A–C) Low magnification shows the histoarchitecture of dorsoventral interpubic transversal sections. (A) The D12 PS fibrocartilaginous disc (FC) attached to metachromatic pads of hyaline cartilage (HC) continuous with the pubic bones (PB) with a cleft between the cartilaginous caps (arrow). (B) On D19, remodeled connective tissues and IpL pseudo-cavity (IpL pc) formation on the relaxed IpL attached to the PB by osteoligamentous junctions (OJ) continuous with the anterior rim that support abdominal orthochromatic muscle fibers (AM). (C) 3 dpp reabsorbed IpL containing central pseudo-cavity (IpL pc), remodeled OJ and PB as well as preserved blood vessels (v) within posterior connective tissue rims (arrow). (D) On D19, recruited mononuclear phagocyte-like cells attached to IpL pc borders (arrowhead) or on inner ECM (black arrow). Insets show details of recruited mononuclear phagocyte-like cells and rarely detected granulocytes near to small blood vessels (v). (E) 3 dpp IpL showing predominantly recruited monocytes or macrophage-like cells (arrow) inside the central IpL pc. Insets show recruited mononuclear phagocyte-like cells with round, dense chromatin nuclei at 3 dpp IpL pc. (A–C) Giemsa staining. (C and D) Hematoxylin-phloxine B staining. (A) Bar = 30 μm. (B) Bar = 200 μm. (C) Bar = 50 μm. (D and E) Bar = 20 μm; Inset scale bar = 10 μm.

by light microscopy and electron microscopy. Histological sections showed dynamic changes in the histoarchitecture during mouse PS remodeling that gives rise to the IpL where the symphyseal spaces or pseudo-cavities are observed (Figure 1A–C). Our results showed that IpL pseudo-cavities lined with interrupted thin-walled cell boundaries that differ from uninterrupted flattened endothelial similar to that observed in the wall of small blood vessels branched around the almost reabsorbed postpartum IpL fibrous rims, without histological evidence of perivascular granulocyte infiltration (Figure 1B–E). Concomitant with IpL expansion and the disentangling of collagen fibers at D19, a Giemsa metachromatic-stained and amorphous substance was observed in the pseudo-cavities (Figure 1B). The well-preserved IpL plastic embedded sections stained with hematoxylin-phloxine B also showed that although polymorphonuclear granulocytes were rarely found near blood vessels mainly at D19 (Figure 1D), recruited mononuclear phagocyte-like cells were observed floating in the IpL pseudo-cavity at the interrupted thin-walled cell boundary of pseudo-cavities and were mainly distributed throughout the IpL ECM at D19 and 3 dpp (Figure 1D and E).

The combination of freeze-fractured IpLs imaged with SEM (Figure 2A and C) and resin-embedded ultrathin sections imaged with transmission electron microscopy (TEM) (Figure 2B and D) provides an additional dimension for studying the presence of IpL-recruited mononuclear phagocyte-like cells from D18 to 3 dpp. While SEM showed internal pseudo-cavity ECM surfaces and the three-dimensional morphology of isolated adhered cells that displayed both a domed round shape and irregular oblong (elongated) shape (Figure 2A and C), TEM showed details of macrophage-like cells that were conspicuously contacting collagen fibers or amorphous, nonfibrillar ECM in IpL pseudo-cavities.

These contacts resulted from interactions between the IpL ECM and small cytoplasmic extensions such as podosomes, the tips of cytoplasmic protrusions such as pseudopods, relatively large vacuoles (macropinosome), or short bleb-like cytoplasmic protrusions mainly in free round cells inside the pseudo-cavities that were most likely lost during SEM preparation (Figure 2B, D, and E). These general aspects of the conspicuous contact between macrophage-like cells and the amorphous ECM or preserved collagen fibril bundles may provide ways by which cells adapt to their displacement and activate endogenous pathways typically associated with tissue remodeling to participate in the accelerated phase of IpL relaxation.

Neu 7/4- and F4/80-positive cells are increased in the interpubic ligament from the end of pregnancy to the early postpartum stage

Since we found recruited mononuclear phagocytes with ultrastructural macrophage features in D18 to 3 dpp IpL samples, we performed immunofluorescence analysis to identify characteristic markers of recruited monocytes and macrophages in interpubic tissues. Immunofluorescence analysis identified cells positive for Neu 7/4 (a monocyte/early differentiated macrophage and neutrophil marker) and F4/80 (a classical macrophage marker) in mouse IpLs from D18 to 3 dpp (Figures 3 and 4). Based on previous observations [28, 34], cervical tissues at 3 dpp were utilized as positive controls for both immunofluorescence assays.

In the D12 PS, few Neu 7/4- or F4/80-positive cells were located inside pubic bones or at pubic bones and hyaline cartilage transitional tissues (Figures 3A and 4A). From late pregnancy to the early postpartum stage, both Neu 7/4- and F4/80-positive mononuclear phagocytes were mainly observed as clusters inside pseudo-cavities along IpL collagen fibers or dispersed in the IpL ECM (Figures 3B–E and 4B–E). As reported above, cells with a characteristic lobed nuclear appearance that were positive for Neu

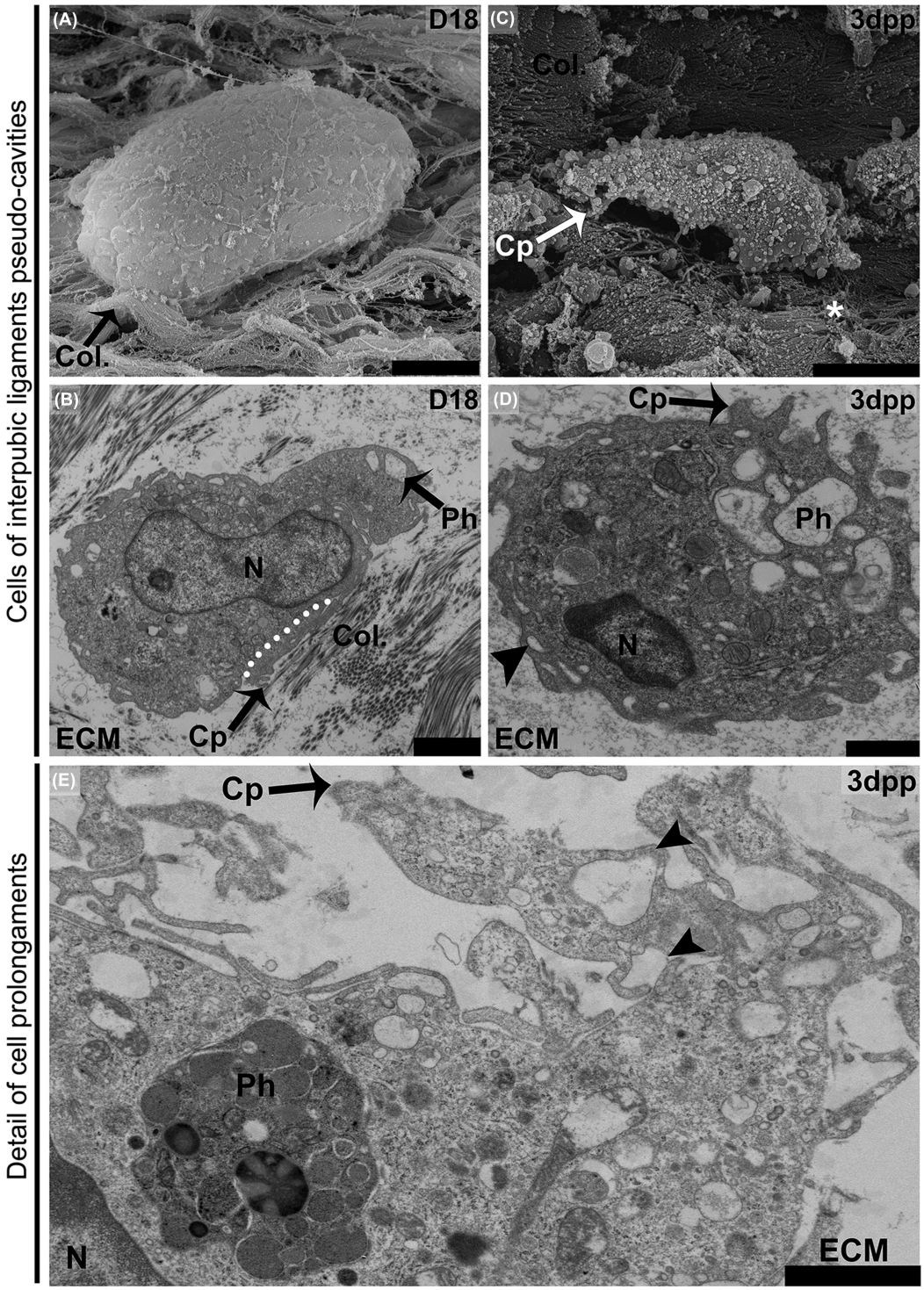

Figure 2. SEM and TEM ultrastructural profiles of recruited mononuclear phagocyte-like cells at lpL pseudo-cavities in remodeled connective tissue at D18 (A and B) and 3 dpp (C–E). (A) At D18, a less differentiated domed, round-shaped cell lining pseudo-cavity exhibiting a slightly wrinkled surface closely associated with scattered bundles of collagen fibrils (Col.) presenting crimped wavy patterns (black arrow). (B) At D18, a more polarized cell surrounded by both amorphous extracellular matrix (ECM) and preserved collagen fibrils was noted (Col.). The cell has an ellipsoid nucleus (N), small phagosomes (Ph), and a cortical cytoplasmic area devoid of organelles (white dotted line). This area has a compact cytoskeleton and short cytoplasmic projections (Cp) associated with aligned collagen fibrils in the ECM. (C) A more differentiated irregular, oblong (elongated)-shaped cell with a deep wrinkled surface at 3 dpp. Note small cytoplasmic projections distributed around the cell periphery (Cp) contacting disrupted collagen fibers containing spread-out thinner fibrils (asterisks). (D) 3 dpp low-density pseudo-cavity with an amorphous gel-like ECM containing a round cell that presents phagosomes (Ph), short bleb-like cytoplasmic projections (Cp), and macropinosome-like (arrowhead) structures at the cell border. (E) 3 dpp cell with features of a phagocytic macrophage-like cell showing phagosomes filled with engulfed materials (Ph) and prominent cytoplasmic projections (Cp) in contact with an amorphous ECM that also forms macropinosome-like structures (arrowheads). (A) Bar = 10 μm. (B, E, and F) Bar = 2 μm. (C) Bar = 5 μm. (D) Bar = 1 μm.

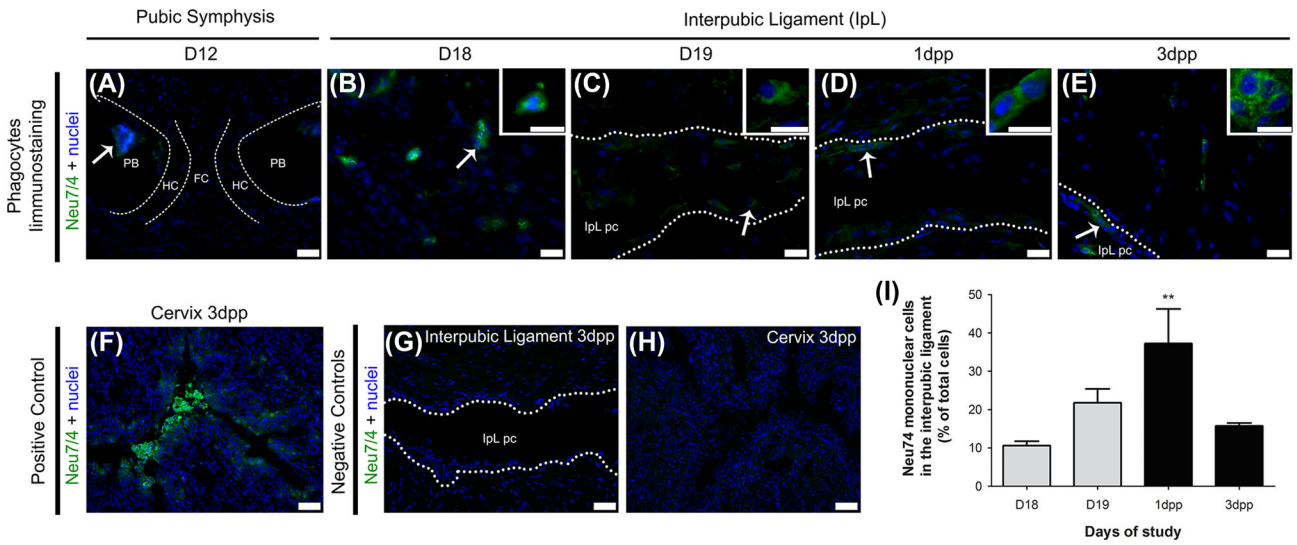

Figure 3. Mononuclear Neu 7/4-positive cell immunolocalization and percentages in the interpubic tissues during remodeling. Photomicrographs of mononuclear cells positive for Neu 7/4 immunofluorescence in the PS (A) and the IpL (B–E) at D12, D18, and D19 of pregnancy and the early postpartum stage. (A) At D12, Neu 7/4-positive mononuclear cells (arrow) were located only in the bone marrow of pubic bones (PB). (B–E) In the IpL, both elongated and round (arrows) mononuclear cells positive for Neu 7/4 were observed in IpL, inside IpL pseudo-cavities (IpL pc) or associated with IpL pc borders (dotted lines) from D18 to 3 dpp. Insets show phenotypic details of mononuclear cells positive for Neu 7/4 in IpL from D18 to 3 dpp. (F) Positive control for Neu 7/4 immunolocalization in mouse cervix at 3 dpp. (G and H) Negative controls were performed without the presence of Neu 7/4 primary antibodies. (I) Semiquantitative analysis of Neu 7/4-positive mononuclear cell percentage variance in the interpubic ligament at the end of pregnancy and early postpartum stage. Quantification of the mean SEM of Neu 7/4-positive mononuclear cells at each time point on 15 images (5 field/section/mouse were analyzed; n = 3; one-way ANOVA with Bonferroni post hoc test, $^{**}P < 0.01$ compared with D18). DAPI staining for nuclei. (A, F–H) Bar = 60 μm (B–E) Bar = 20 μm.; Inset scale bar = 10 μm.

7/4 were rare in interpubic tissues from D12 to 3 dpp, representing 1–2% of the total cell population in the IpL from D18 to 3 dpp (data not shown).

Similar to the TEM and SEM analyses, Neu 7/4- or F4/80-positive mononuclear phagocytes exhibited distinct morphologies according to their localization in the IpL. Whereas elongated cells positive for both markers were observed either at the periphery of IpL pseudo-cavities or in contact with the IpL EMC, round Neu 7/4- or F4/80-positive cells were located only inside IpL pseudo-cavities and near pubic bones. These changes in morphological profiles may not be related to time since both cell morphologies could be observed from D18 to 3 dpp. Cervical tissues at 3 dpp were a consistent positive control for the immunofluorescence assays (Figures 3F and 4F).

Semiquantitative analyses of the percentage of mononuclear Neu 7/4- and F4/80-positive cells in interpubic tissues showed that both populations gradually increased in the IpL from the end of pregnancy (10.6% of Neu7/4$^+$ cells at D18 and 21.8% of Neu7/4$^+$ cells at D19; 17.2% of F4/80$^+$ cells at D18 and 24.2% of F4/80$^+$ cells at D19) to 1 dpp (37.3% of Neu7/4$^+$ cells and 28.9% of F4/80$^+$ cells) when Neu 7/4-positive cells achieved their highest percentage in the IpL (Figures 3I and 4I). At 3 dpp, while the percentage of Neu7/4-positive cells decreased (15.7%), F4/80-positive cells were present at their highest percentage (40.7%) in the IpL (Figures 3I and 4I).

Dynamic changes in the macrophage phenotype and the expression of anti-inflammatory and proinflammatory macrophage-related genes play a role in interpubic tissue remodeling

The double immunofluorescence for M1 (F4/80$^+$/CD40$^+$) and M2 (F4/80$^+$/TfR$^+$) macrophage markers [45, 46] showed different macrophage activation phenotypes in interpubic tissues from D18 to 3 dpp (Figure 5). Similar to our F4/80 immunolocalization, TEM, and SEM results, both elongated and round macrophages were observed in IpL pseudo-cavities and the IpL ECM from D18 to 3 dpp (Figure 5A–H). Both elongated and round phagocytes localized at IpL were positive for either M1 or M2 phenotype markers from D19 to 3 dpp (Figure 5B–D and F–H). However, it is notable that double-positive cells for M1 and M2 markers were rare in the IpL on D18 (Figure 5A and E). These results underscore the fact that both active M1 and M2 macrophage phenotypes are present in the IpL during both its relaxation before labor and during early PS postpartum recovery.

Furthermore, we analyzed temporal changes in the relative gene expression levels of migratory monocyte (*Ccr2*) and macrophage (*F4/80*) markers, inflammatory response cytokines and M1 markers (*Tnf-alpha* and *Il1a*), and M2 (*Tgf-beta*, *Arg1*, and *Il10*) macrophage activity by real-time PCR from D18 to 3 dpp (Figure 5M–S). The relative gene expression levels of both *Ccr2* and *F4/80* gradually increased from the end of pregnancy until the early postpartum stage (Figure 5M and N). Concerning M1- and M2-related genes at the end of pregnancy (D18, D19), only the relative gene expression level of *Arg1* increased in the interpubic tissues when compared with that at D12 (Figure 5P). However, the relative gene expression levels of both *Il10* and *Tnf-alpha* at D12 were restored at D19 (Figure 5Q and R). Unlike the expression levels of *IL10, Tnf-alpha,* and *IL1a*, which increased during postpartum recovery (Figure 5Q–S), the relative gene expression level of *Arg1* drastically decreased at 1 dpp (Figure 5p). At 3 dpp, the relative gene expression levels of *IL1a* and *Tnf-alpha* were maintained (Figure 5R and S), and those of *Arg1* and *Tgf-beta* increased when compared to those at 1 dpp, with levels returning to those observed at D18 and D12, respectively (Figure 5P and O). Taken together, these data show a gradual increase in macrophage

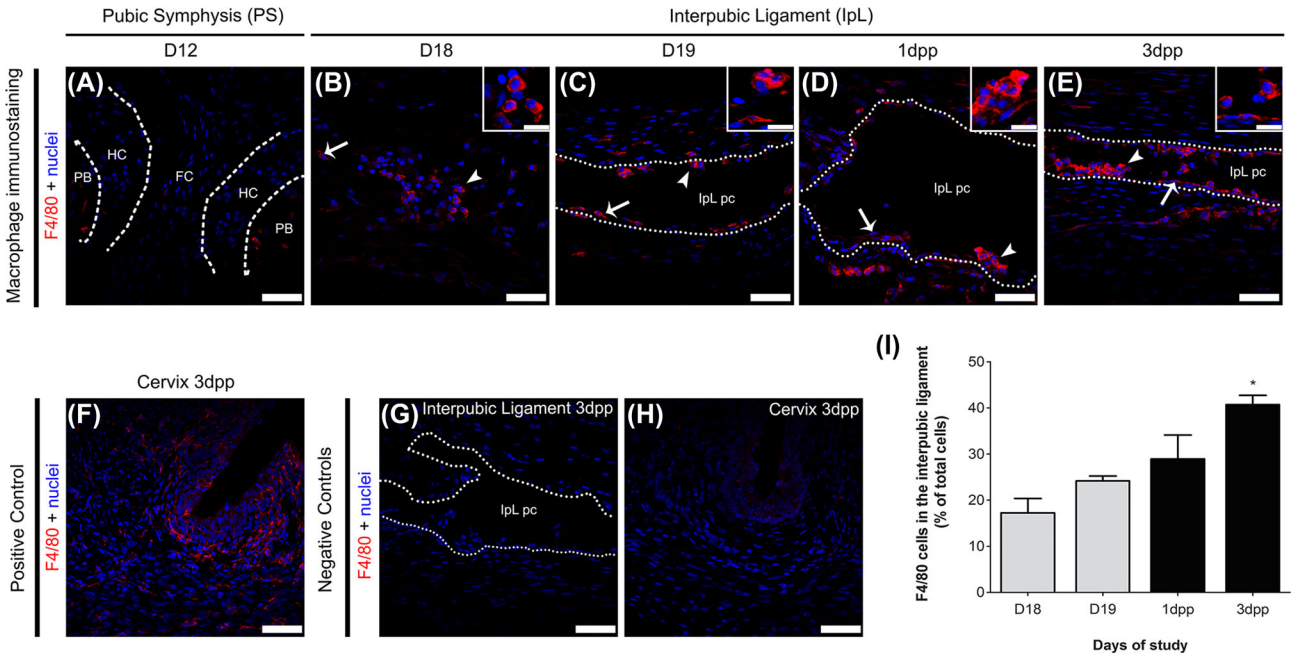

Figure 4. F4/80-positive cell immunolocalization in the interpubic tissues during pregnancy and postpartum recovery. Photomicrographs of positive cells for F4/80 immunofluorescence in the PS (A) and the IpL (B–E) during pregnancy and the early postpartum stage. (A) F4/80-positive cells were located in pubic bones (PB) and not at hyaline cartilage (HC) or fibrocartilage tissues (FC) in the D12 PS. (B–E) At the interpubic ligament, both elongated (arrows) and round (arrowheads) cells positive for F4/80 were observed in IpL, inside IpL pseudo-cavities (IpL pc) or associated with IpL pc borders (dotted lines) from D18 to 3 dpp. Insets show phenotypic details of mononuclear cells positive for F4/80 in IpL from D18 to 3 dpp. (F) Positive control for F4/80 expression in mouse cervix at 3 dpp. (G and H) Negative controls were performed without the presence of F4/80 primary antibodies. (I) Semiquantitative analysis of F4/80-positive cell percentage variance in the interpubic ligament at the end of pregnancy and early postpartum stage. Quantification of the mean SEM of F4/80-positive cells at each time point on 15 images (5 field/section/mouse were analyzed; n = 3; one-way ANOVA with Bonferroni post hoc test, $^{*}P < 0.05$ compared with D18). DAPI staining for nuclei. (A–H) Bar = 30 μm; Insets scale bar = 15 μm.

and monocyte migration markers, followed by dynamic changes in M1- and M2-related inflammatory modulator gene expression levels from D18 to 3 dpp.

Discussion

Our findings identify the presence of recruited mononuclear phagocytes in mouse interpubic tissue during its full relaxation at labor and its repair during postpartum recovery. Semiquantitative analysis of cells immunolabeled for specific monocyte/macrophage markers showed that the number of recruited monocytes is increased in interpubic tissues, and that these recruited monocytes differentiate into proinflammatory ($F4/80^{+}/CD40^{+}$) or anti-inflammatory ($F4/80^{+}/TfR^{+}$) macrophage phenotypes from D18 to 3 dpp, which may contribute to dynamic changes in the gene expression of specific inflammatory mediators involved in interpubic tissue remodeling at these time points. Therefore, these cells may act as activated and polarized macrophages that might help both in IpL relaxation for successful labor and promotion of the appropriate recovery of mouse PS histoarchitecture after the first pregnancy.

Light microscopy findings illustrate widely recognized aspects of the accelerated phase of IpL relaxation during the end of pregnancy and PS postpartum recovery [4, 13, 14, 27]. Additionally, as previously described in rats by Rocha and Chopard [47], the small diameter blood vessels inside of the IpL anterior and posterior connective tissue rims observed in our resin-embedded section from D18 to 3 dpp may be taken as clear evidence of fast remodeling to offer PS nutritional support, which is particularly important for reproductive tract homeostasis [47].

Furthermore, pseudo-cavities filled with a metachromatic amorphous substance and cells were identified in the IpL in our resin-embedded histological data. Although general similarities are shared between these structures and the IpL sinusoidal like-cavities, intercommunicating channels or symphyseal space of the indistinct edge found in early studies of mouse, guinea pig, and human PS remodeling [13, 14, 29, 48]. The presence of recruited mononuclear phagocyte-like cells inside or at the borders of the IpL pseudo-cavities differs from the early description of those cells, as fibroblasts that have migrated to symphyseal space edges and swollen chondrocytes that appear to be migrating into the space [14]. They also differ from osteoclasts located primarily at the periphery of the mouse pubic bones but not in the loose or fluid, relaxed IpL [17, 18], and do not resemble an increased angiogenesis that supports a heavy polymorphonuclear and mononuclear leukocyte invasion as observed in PS guinea pig from midpregnancy (D49) to parturition [29].

Both our SEM and TEM results showed that recruited mononuclear phagocyte-like cells in pseudo-cavities had ultrastructural macrophage features similar to those described by classical electron microscopy studies of monocytes to macrophage differentiation in vitro [49] and the more recent characterization of three dimensional human macrophage migration [50]. Moreover, these ultrastructural features, such as phagosomes filled with engulfed materials, prominent cytoplasmic extensions that project multiple pseudopods with

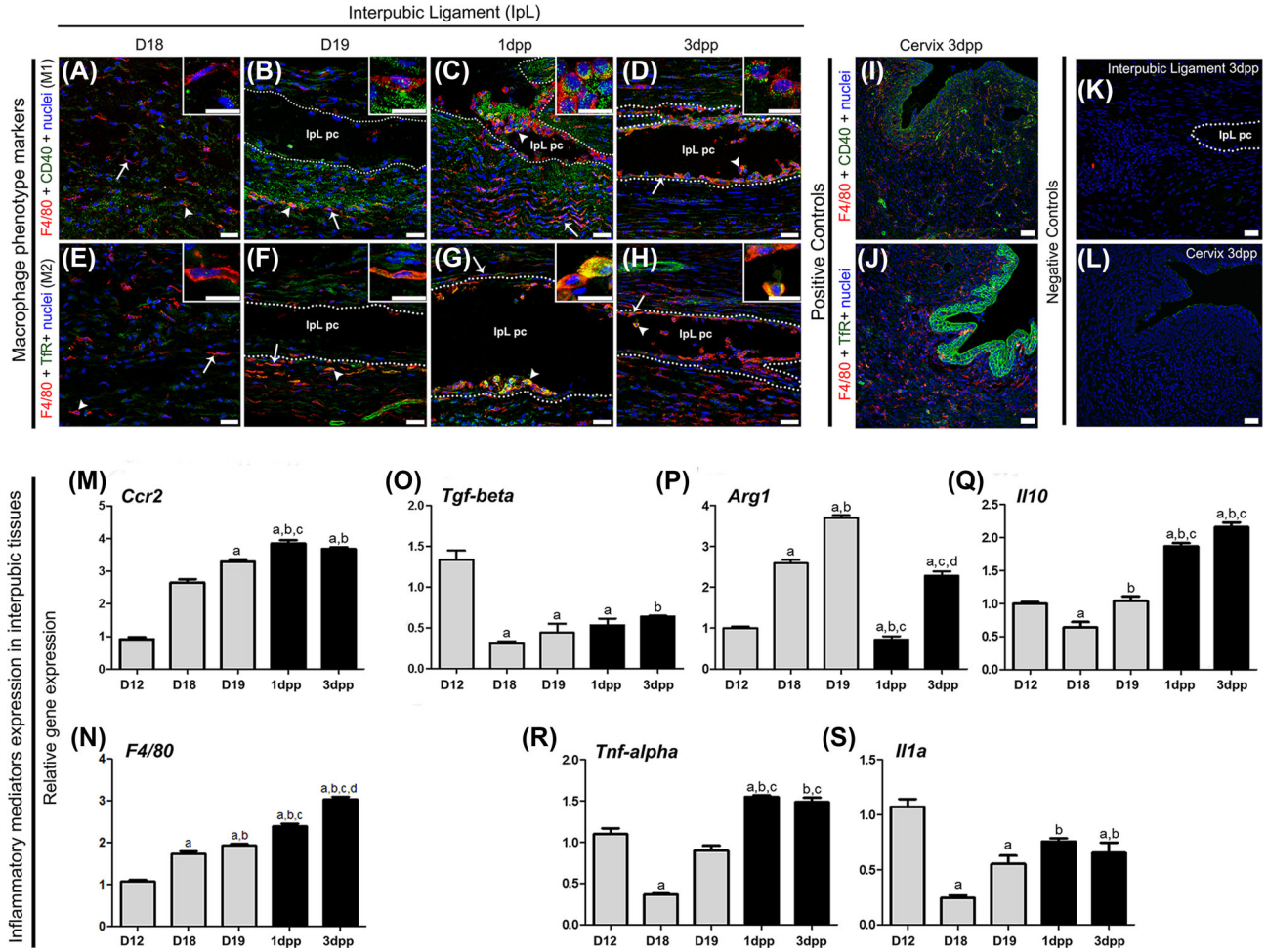

Figure 5. Immunolocalization of M1 and M2 macrophage phenotypes and quantitative real-time PCR analysis of genes related to monocyte migration and macrophage activity in interpubic tissue remodeling. (A–H) Elongated (arrows) and round (arrowheads) cells double positive for F4/80 and CD40 (A–D) or for F4/80 and transferrin receptor (TfR) (E–H) were observed in IpL fibrillar extracellular matrix (IpL EMC), inside IpL pseudo-cavities (IpL pc) or associated with IpL pc borders (dotted lines) mainly from D19 to 3 dpp. Insets show details of M1 (A–D) and M2 (E–H) phenotypes F4/80 and CD40 or for F4/80 and TfR (E–H) in IpL tissues from D18 to 3 dpp. (I and J) Positive control for F4/80 expression in the mouse cervix at 3 dpp. (K and L) Negative controls were analyzed without the presence of primary antibodies. (M and N) Expression of the monocyte migration marker Ccr2 and macrophage marker F4/80 progressively increased after D18. (O–S) M2 (*Tgf-beta*, *Arg1*, and *Il10*) and M1 (*Tnf-alpha* and *Il1a*)-related cytokines and molecules showed dynamic expression during pregnancy and postpartum recovery. Statistical data analysis was performed by one-way ANOVA with the Tukey post hoc test, and the data represent the mean ± SEM from six (D12 and 3 dpp) or three (D18, D19, and 1 dpp) interpubic tissues with significance ($P < 0.05$) indicated by: a, compared with D12; b, compared with D18; c, compared with D19; and d, compared with 1 dpp. (A–L) Bars = 30 μm. Inset scale bar = 15 μm.

variable lengths, and macropinosomes, are consistent with a previous described "peculiar cell-type" that was assumed to be responsible for PS remodeling and contribute to pseudo-cavity development in the IpL in the final days of pregnancy [38] that, to our knowledge, was the only previous ultrastructural characterization of macrophage-like cells in the mouse PS.

Although our SEM and TEM results represent only cell attachments at the moment of fixation, the contact between macrophage-like cells and fibrillary or amorphous ECM components signals displacement within a highly porous fibrillary collagen network or even at the surface of the pseudo-cavities, where cells with a domed round shape or oblong and protrusive phenotype are attached. The contacts between both cell phenotypes, also shown by our immunofluorescent assays as round or elongated cells, and collagens fibrils by podosome-like cell projections or the amorphous IpL pseudo-cavity ECM by pseudopod tips are consistent with the idea that macrophage-like cells present in the mouse IpL environment during drastic and fast remodeling probably undergo changes from amoeboid (protease-independent) to mesenchymal (protease-dependent) migratory phenotypes in response to intracellular or ECM dynamic changes [50–52]. Additionally, once polarized macrophages present distinct cell shapes in vitro [53], the presence of both round and elongated phagocyte-like cells in IpL may indicate that distinct activated macrophage phenotypes are present in IpL from late pregnancy to postpartum.

Moreover, the presence of macropinosome-like structures in IpL macrophage-like cells observed by TEM may indicate that they actively participate in ECM remodeling because these structures enable macrophages to sample their environment and mediate nonselective fluid-phase uptake from the ECM environment by macropinocytic cups, giving rise to large macropinosome vacuoles that, after maturation, are fused with lysosomes for degradation [54]. In

accordance with that hypothesis, the intense loss of clearance presented by double-knockout animals for both macrophage scavenger receptors ManR and AsgR lead to loss of interpubic tissue homeostasis during late pregnancy [55]. Among them, 61% of the pregnant mice failed to relax the IpL to initiate parturition at the evening of D19 and died when parturition was initiated at a later time [55], uncovering an important role of macrophages in drastic interpubic tissue remodeling for safe delivery.

Immunostaining analyses for myeloid cell markers allowed us to confirm that recruited mononuclear phagocyte populations described by light microscopy and electron microscopy were both monocytes/recently activated macrophages (Neu7/4) or mature polarized macrophages ($F4/80^+/CD40^+$ and $F4/80^+/TfR^+$). The increase in Neu7/4- and F4/80-positive cells observed in the IpL during the end of pregnancy and during postpartum recovery is similar to the temporal dynamic described for macrophages in other female lower reproductive tract and pelvic floor structures such as uterine, cervical, and adipose parametrial tissues [5, 28, 32, 34]. Those macrophages differ from osteoclasts by their localization in IpL where osteoclasts are located primarily at the periphery of the mouse pubic bones [17, 18] and IpL macrophages were seen at IpL ECM and pseudo-cavities, and by IpL macrophage positive immunostaining for F4/80, since the F4/80 molecule suppress osteoclast differentiation [56]. With respect to granulocytes, our histological and Neu 7/4 immunostaining results confirmed previous observations, showing that they were rarely found in interpubic tissues without signals of the infiltration process from D12 to 3 dpp [21, 26]. The prevalence of recruited mononuclear phagocytes in the mouse IpL during pregnancy emphasizes the distinction between the mouse and guinea pig in terms of the requirement of granulocytes for interpubic tissue relaxation during labor [29].

Consistent with Neu 7/4 immunostaining, our qPCR results showed the increased mRNA expression of monocyte receptor *Ccr2* from the end of pregnancy up to 1 dpp. Bearing in mind the critical role of this chemokine receptor in the mobilization and recruitment of monocytes from bone marrow to sites of inflammation [57] and that the 7/4-antigen, which is synonymous with the Ly-6B.2 alloantigen, may serve as a useful surrogate marker for recently recruited monocyte-derived inflammatory macrophages in an inflammatory context [58], the correlation between the increase in *Ccr2* expression levels and Neu7/4-positive cells in the IpL may indicate the existence of mechanisms related to the modulation of monocyte migration and to their fast differentiation into macrophages in interpubic tissue remodeling from the end of pregnancy to the early postpartum stage.

Similar to observations in uterine tissues, where macrophages play a key role in the clearance of senescent uterine cells to maintain postpartum uterine function [32], particularly during postpartum PS recovery there was an increase in relative F4/80 expression levels and the number of immunoassayed cells in the IpL. These $F4/80^+$ cells were also positive for the novel markers of M1 and M2 macrophage polarization phenotype [45]: CD40, which can trigger macrophage expression and the production of proinflammatory molecules such as *Tnf-alpha* [59] and NOS2 [60], or TfR, which is typically upregulated in mouse M2 macrophages [46]. Coincidently, particularly during labor and postpartum PS recovery, the increase in Neu 7/4 and F4/80 cell percentage in the IpL was followed not only by an increase in the expression levels of F4/80 but also by an increase in expression levels of the inflammatory mediators *Il10*, *Il1a,* and *Tnf-alpha,* which are markers of the M1/M2 polarized activation states of macrophages [61]. These findings suggest that the recently differentiated $Neu7/4^+$ macrophages became mature and probably polarized macrophages during mouse interpubic tissue remodeling.

As suggested by the identification of elongated and round macrophage-like cells by our light and electron microscopy analysis, our qPCR and immunostaining results showed that a mixed population of macrophages displaying phenotypes across both extremes of polarization state has evolved to ensure optimal interpubic tissue remodeling during pregnancy, as described in the uterine cervix [2, 28, 33], decidua [31, 35], and parametrial adipose tissue [5]. At the end of pregnancy, the localization of $F4/80^+/CD40^+$ cells and the progressive increase in M1 polarization marker (*Tnf-alpha* and *Il1a)* expression shown in this work are consistent with previous findings concerning the increase in *iNos* expression levels and NO production in mouse interpubic tissues [24], indicating that M1 macrophages can contribute to IpL relaxation at labor, thereby contributing to optimal accommodation by the mouse female lower reproductive tract and safe delivery. The upregulation of *Il10* and *Arg1* mRNA expression and the presence of $F4/80^+/TfR^+$ cells during the end of pregnancy and postpartum recovery in this investigation suggest that M2 macrophages are also likely actively engaged in interpubic tissue remodeling.

As detailed by Zhang and coworkers [35], macrophage polarization is triggered by signals present in the surrounding environment accompanied by a set of signaling pathways and transcriptional and posttranscriptional regulatory networks. M1/M2 polarization is strongly related to the *iNOS* and arginase pathways, respectively [31, 35], and the decrease in *Arg1* levels in interpubic tissues may be indicative of the prevalence of the M1 phenotype at the beginning of postpartum repair. Although this proposition agrees with the peak *Il1a* and *Tnf-alpha* expression levels detected at 1 dpp, maximal *Il10* expression levels observed at 1 dpp and 3 dpp have the potential to trigger compensatory mechanisms in M1 cells in response to M2 phenotype cell activation, as observed in parametrial adipose tissue during late pregnancy [5]. Additionally, unlinked cell culture experiments [53], the presence of both elongated and round macrophages positive for M1 and M2 markers in IpL indicates that, in this specific tissue remodeling microenvironment, a more complex macrophage polarization spectra may be necessary to guarantee tissue homeostasis. This balance between proinflammatory and anti-inflammatory mediators is crucial to develop a process that could be considered "orderly" inflammation necessary for the activation of the wound-healing response and for tissue homeostasis to be restored [62], which seem to be essential to proper remodeling of the IpL since mouse $LOXL1^{-/-}$ pelvic floor disorders after parturition are associated with both increased proinflammatory cytokine production at the pelvic organs [63] and exacerbated interpubic tissue relaxation during labor [12].

The presence of high expression levels of both pro- and anti-inflammatory mediators associated with $F4/80^+/TfR^+$-positive cells in interpubic tissues from 1 dpp may also be indicative of M2 subtype or M2-like macrophages during postpartum recovery. The M2 macrophages can be divided into subcategories (M2a, M2b, M2c, and M2d) based on both the type of agonists responsible for triggering their differentiation and the distinct functional profile induced by these agonists [31, 64]. Consistent with our results regarding M1/M2 polarization marker gene expression in the mouse IpL during postpartum recovery, M2d mouse peritoneal macrophages express high levels of *Il10* and *iNOS* and low levels of *Tnf-alpha* and *Arg1* intermediates [65], and M2b macrophages are able to secrete *Tnf-alpha* when influenced by proinflammatory cytokines [31]. Thus, the

profile of macrophage polarization markers measured at 1 dpp and 3 dpp in interpubic tissues may suggest a switch of M2 macrophages to M2-like phenotypes capable of proinflammatory cytokine secretion, which can occur rapidly and reversibly according to changes in cytokines in the environment [35, 66]. Together with M1 macrophages, these cells may help to increase proinflammatory mediator secretion in the IpL during the postpartum period but still be able to produce anti-inflammatory molecules such as *Il10* and *Arg1* that regulate the immune response during this process.

Finally, at 3 dpp, despite the maintenance of high expression levels of proinflammatory cytokines, our results showed increases in the relative expression levels of *Arg1, Il10,* and *Tgf-beta* in interpubic tissues when compared with those at 1 dpp. The increase in anti-inflammatory mediator expression levels at 3 dpp can be associated with the beginning of the tissue repair process, similar to that observed in wound healing [62] and in vitro models to explain the role of monocytes in modulating myometrial inflammation after labor onset [67], leading to the amount of inflammation necessary for the reestablishment of tissue homeostasis. Corroborating that hypothesis, it was previously reported that intense ECM reorganization associated with the differentiation of fibroblasts into myofibroblasts occurred at the early postpartum stage [27, 68], which resulted in hyaline cartilage recovery after 10 dpp [16] and the return to a similar nonpregnant PS structure after 40 dpp after the first pregnancy [26].

In summary, our data may provide evidence that changes in the mouse PS from the end of pregnancy to the postpartum stage may be influenced by recruited monocyte differentiation and the macrophage state of activation, which may give rise to a process associated with an "orderly" inflammation mechanism. F4/80-positive macrophages that also showed positive immunofluorescence for M1 or M2 markers present in the IpL ECM and pseudo-cavities from D18 to 3 dpp could be considered to be differentiated macrophages that most likely contribute to dynamic changes in inflammatory mediators gene expression seen in interpubic tissues at the same time points and help to orchestrate tissue remodeling during IpL relaxation for labor and in postpartum PS recovery. Therefore, our data suggest a model in which monocyte recruitment and macrophage heterogeneity facilitate the efficient recovery and repair of the PS after birth, thus ensuring mechanical stability for the reproductive tract and the ability to initiate and maintain a subsequent pregnancy.

Future studies will be necessary to identify in vivo endogenous molecular signals in the IpL that may help to control myeloid cell recruitment and state of activation during late pregnancy and fast postpartum interpubic tissue remodeling to better understand the molecular mechanisms involved in this joint as it returns to homeostasis in the mouse animal model.

Supplementary data

Supplementary data are available at *BIOLRE* online.

Supplemental Table S1. Primers used in the present work.

Acknowledgments

We thank Mainara Barbieri and Natália Roberta dos Santos for excellent technical assistance, Dr Lúcia Elvira Alvares for permission to use the Developmental Biology Laboratory, Dr Alexandre Leite Rodrigues de Oliveira for permission to use the Leica DM5500B microscope in the Laboratory of Nerve Regeneration and the INFABIC at UNICAMP for access to Zeiss LSM780-NLO confocal microscopy. We also acknowledge the Biological Imaging facility LNBio and Electron Microcopy Laboratory at LNNano (CNPEM, Campinas, Brazil) for their support with the use of confocal (Leica TCS SP8) and electron (FEI Quanta 650 FEG) microscopies.

References

1. Sherwood O. Relaxin. In: Neill EKaJD (ed.) *The Physiology of Reproduction*, 2nd edn. New York: Raven Press; 1994: 861–1009.
2. Mahendroo M. Cervical remodeling in term and preterm birth: insights from an animal model. *Reproduction* 2012; **143**(4):429–438.
3. Shynlova O, Mitchell JA, Tsampalieros A, Langille BL, Lye SJ. Progesterone and gravidity differentially regulate expression of extracellular matrix components in the pregnant rat myometrium. *Biol Reprod* 2004; **70**(4):986–992.
4. Dhital B, Gul ENF, Downing KT, Hirsch S, Boutis GS. Pregnancy-Induced dynamical and structural changes of reproductive tract collagen. *Biophys J* 2016; **111**(1):57–68.
5. Zhang L, Sugiyama T, Murabayashi N, Umekawa T, Ma N, Kamimoto Y, Ogawa Y, Sagawa N. The inflammatory changes of adipose tissue in late pregnant mice. *J Mol Endocrinol* 2011; **47**(2):157–165.
6. Akgul Y, Holt R, Mummert M, Word A, Mahendroo M. Dynamic changes in cervical glycosaminoglycan composition during normal pregnancy and preterm birth. *Endocrinology* 2012; **153**(7):3493–3503.
7. Ruscheinsky M, De la Motte C, Mahendroo M. Hyaluronan and its binding proteins during cervical ripening and parturition: dynamic changes in size, distribution and temporal sequence. *Matrix Biol* 2008; **27**(5):487–497.
8. Alperin M, Debes K, Abramowitch S, Meyn L, Moalli PA. LOXL1 deficiency negatively impacts the biomechanical properties of the mouse vagina and supportive tissues. *Int Urogynecol J* 2008; **19**(7):977–986.
9. Drewes PG, Yanagisawa H, Starcher B, Hornstra I, Csiszar K, Marinis SI, Keller P, Word RA. Pelvic organ prolapse in fibulin-5 knockout mice. *Am J Pathol* 2007; **170**(2):578–589.
10. Lee UJ, Gustilo-Ashby AM, Daneshgari F, Kuang M, Vurbic D, Lin DL, Flask CA, Li T, Damaser MS. Lower urogenital tract anatomical and functional phenotype in lysyl oxidase like-1 knockout mice resembles female pelvic floor dysfunction in humans. *Am J Physiol Renal Physiol* 2008; **295**(2):F545–F555.
11. Rahn DD, Acevedo JF, Roshanravan S, Keller PW, Davis EC, Marmorstein LY, Word RA. Failure of pelvic organ support in mice deficient in fibulin-3. *Am J Pathol* 2009; **174**(1):206–215.
12. Borazjani A, Couri B, Balog B, Damaser M. Mp1-13 Pubic symphysis length is correlated with pelvic organ prolapse in lysyl oxidase like-1 knockout mice. *J Urol* 2014; **191**(4S):e6.
13. Hall K. Changes in the bone and cartilage of the symphysis pubis of the mouse during pregnancy and after parturition, as revealed by metachromatic staining and the periodic Acid-Schiff technique. *J Endocrinol* 1954; **11**(2):210–222.
14. Storey E. Relaxation in the pubic symphysis of the mouse during pregnancy and after relaxin administration, with special reference to the behaviour of collagen. *J Pathol*. 1957; **74**(1):147–162.
15. Crelin ES. The development of the bony pelvis and its changes during pregnancy and parturition. *Trans NY Acad Sci* 1969 **31**(8 Series II):1049–1058.
16. Castelucci BG, Consonni SR, Rosa VS, Sensiate LA, Delatti PCR, Alvares LE, Joazeiro PP. Time-dependent regulation of morphological changes and cartilage differentiation markers in the mouse pubic symphysis during pregnancy and postpartum recovery. *PLoS One* 2018; **13**(4):e0195304.
17. Steinetz BG, Matthews JR, Butler MC, Thompson SW, 2nd. Inhibition by thyrocalcitonin of estrogen-induced bone resorption in the mouse pubic symphysis. *Am J Pathol* 1973; **73**:735–746.
18. McDonald JK, Schwabe C. Relaxin-induced elevations of cathepsin B and dipeptidyl peptidase I in the mouse pubic symphysis, with localization

by fluorescence enzyme histochemistry. *Ann NY Acad Sci* 1982; **380**(1 Relaxin):178–186.
19. Moraes SG, Pinheiro MC, Toledo OMS, Yamada AT, Joazeiro PP. Differential distribution of elastic system fibers in the pubic symphysis of mice during pregnancy. *Braz J morphol Sci* 2003; **20**(2):85–92.
20. Consonni SR, Werneck CC, Sobreira DR, Kuhne F, Moraes SG, Alvares LE, Joazeiro PP. Elastic fiber assembly in the adult mouse pubic symphysis during pregnancy and postpartum. *Biol Reprod* 2012; **86**: 151, 151–110.
21. Rosa RG, Tarsitano CA, Hyslop S, Yamada AT, Toledo OM, Joazeiro PP. Relaxation of the mouse pubic symphysis during late pregnancy is not accompanied by the influx of granulocytes. *Microsc Res Tech* 2008; **71**:169–178.
22. Rosa RG, Tarsitano CA, Hyslop S, Yamada AT, Toledo OM, Joazeiro PP. Temporal changes in matrix metalloproteinases, their inhibitors, and cathepsins in mouse pubic symphysis during pregnancy and postpartum. *Reprod Sci* 2011; **18**:963–977.
23. Rosa RG, Akgul Y, Joazeiro PP, Mahendroo M. Changes of large molecular weight hyaluronan and versican in the mouse pubic symphysis through pregnancy. *Biol Reprod* 2012; **86**:44.
24. Moro CF, Consonni SR, Rosa RG, Nascimento MA, Joazeiro PP. High iNOS mRNA and protein localization during late pregnancy suggest a role for nitric oxide in mouse pubic symphysis relaxation. *Mol Reprod Dev* 2012; **79**:272–282.
25. Pinheiro M. Ultrastructural and immunohistochemical analysis of proteoglycans in mouse pubic symphysis. *Cell Biol Int* 2003; **27**:647–655.
26. Consonni SR, Rosa RG, Nascimento MAC, Vinagre CM, Toledo OMS, Joazeiro PP. Recovery of the pubic symphysis on primiparous young and multiparous senescent mice at postpartum. *Histol Histopathol* 2012; **27**:885–896.
27. Joazeiro PP, Consonni SR, Rosa RG, Toledo OMS. Peri-Partum changes to mouse pubic symphysis. In: Croy A, Yamada AT, DeMayo FJ, Adamson SL (eds.), *The Guide to Investigation of Mouse Pregnancy*. 1st edn. USA: Elsevier Inc; 2014:403–417.
28. Timmons BC, Fairhurst AM, Mahendroo MS. Temporal changes in myeloid cells in the cervix during pregnancy and parturition. *J Immunol* 2009; **182**:2700–2707.
29. Rodriguez HA, Ortega HH, Ramos JG, Munoz-de-Toro M, Luque EH. Guinea-pig interpubic joint (symphysis pubica) relaxation at parturition: underlying cellular processes that resemble an inflammatory response. *Reprod Biol Endocrinol* 2003; **1**:113.
30. Shynlova O, Nedd-Roderique T, Li YQ, Dorogin A, Nguyen T, Lye SJ. Infiltration of myeloid cells into decidua is a critical early event in the labour cascade and post-partum uterine remodelling. *J Cell Mol Med* 2013; **17**:311–324.
31. Brown MB, von Chamier M, Allam AB, Reyes L. M1/M2 macrophage polarity in normal and complicated pregnancy. *Front Immunol* 2014; **5**:606.
32. Egashira M, Hirota Y, Shimizu-Hirota R, Saito-Fujita T, Haraguchi H, Matsumoto L, Matsuo M, Hiraoka T, Tanaka T, Akaeda S, Takehisa C, Saito-Kanatani M et al. F4/80+ macrophages contribute to clearance of senescent cells in the mouse postpartum uterus. *Endocrinology* 2017; **158**:2344–2353.
33. Yellon SM. Contributions to the dynamics of cervix remodeling prior to term and preterm birth. *Biol Reprod* 2017; **96**:13–23.
34. Payne KJ, Clyde LA, Weldon AJ, Milford TA, Yellon SM. Residency and activation of myeloid cells during remodeling of the prepartum murine cervix. *Biol Reprod* 2012; **87**:106.
35. Zhang YH, He M, Wang Y, Liao AH. Modulators of the balance between M1 and M2 macrophages during pregnancy. *Front Immunol* 2017; **8**:120.
36. Mackler AM, Iezza G, Akin MR, McMillan P, Yellon SM. Macrophage trafficking in the uterus and cervix precedes parturition in the mouse. *Biol Reprod* 1999; **61**:879–883.
37. Yellon SM, Greaves E, Heuerman AC, Dobyns AE, Norman JE. Effects of macrophage depletion on characteristics of cervix remodeling and pregnancy in CD11b-dtr mice. *Biol Reprod* 2019; **100**(5):1386–1394.
38. Linck G, Petrovic A, Stoeckel ME, Porte A. Fine structure of the public symphysis in the mouse. *Bull Assoc Anat (Nancy)*. 1976; **60**:201–209.
39. Bennett HS, Wyrick AD, Lee SW, McNeil JH. Science and art in preparing tissues embedded in plastic for light microscopy, with special reference to glycol methacrylate, glass knives and simple stains. *Stain Technol* 1976; **51**:71–97.
40. Joazeiro PP, Consonni SR, Rosa RG, Toledo OMS. Pubic symphysis evaluation. In: Croy A, Yamada AT, DeMayo FJ, Adamson SL (eds.), *The Guide to Investigation of Mouse Pregnancy*. 1st edn. USA: Elsevier Inc; 2014:733–750.
41. Heuerman AC, Hollinger TT, Menon R, Mesiano S, Yellon SM. Cervix stromal cells and the progesterone receptor a isoform mediate effects of progesterone for prepartum remodeling. *Reprod Sci* **2019**:1933719118820462.
42. Schneider CA, Rasband WS, Eliceiri KW. NIH Image to ImageJ: 25 years of image analysis. *Nat Methods* 2012; **9**:671–675.
43. Conover WJ, Iman RL. Rank transformations as a bridge between parametric and nonparametric statistics. *Am Stat* 1981; **35**:124–129.
44. Montgomery DC. *Design and Analysis of Experiments*. New York: John Wiley & Sons.; 1991.
45. Becker L, Liu NC, Averill MM, Yuan W, Pamir N, Peng Y, Irwin AD, Fu X, Bornfeldt KE, Heinecke JW. Unique proteomic signatures distinguish macrophages and dendritic cells. *PLoS One* 2012; **7**:1–12.
46. Corna G, Campana L, Pignatti E, Castiglioni A, Tagliafico E, Bosurgi L, Campanella A, Brunelli S, Manfredi AA, Apostoli P, Silvestri L, Camaschella C et al. Polarization dictates iron handling by inflammatory and alternatively activated macrophages. *Haematologica* 2010; **95**:1814–1822.
47. da Rocha RC, Chopard RP. Nutrition pathways to the symphysis pubis. *J Anatomy* 2004; **204**:209–215.
48. Putschar WG. The structure of the human symphysis pubis with special consideration of parturition and its sequelae. *Am J Phys Anthropol* 1976; **45**:589–594.
49. Sutton JS, Weiss L. Transformation of monocytes in tissue culture into macrophages epithelioid cells and multinucleated giant cells - an electron microscope study. *J Cell Biol* 1966; **28**:303–332.
50. Van Goethem E, Poincloux R, Gauffre F, Maridonneau-Parini I, Le Cabec V. Matrix architecture dictates three-dimensional migration modes of human macrophages: differential involvement of proteases and podosome-like structures. *J Immunol* 2010; **184**:1049–1061.
51. Lammermann T, Germain RN. The multiple faces of leukocyte interstitial migration. *Semin Immunopathol* 2014; **36**:227–251.
52. Cermak V, Gandalovicova A, Merta L, Fucikova J, Spisek R, Rosel D, Brabek J. RNA-seq of macrophages of amoeboid or mesenchymal migratory phenotype due to specific structure of environment. *Sci Data* 2018; **5**:180198.
53. McWhorter FY, Wang T, Nguyen P, Chung T, Liu WF. Modulation of macrophage phenotype by cell shape. *Proc Natl Acad Sci USA* 2013; **110**:17253–17258.
54. Egami Y. Molecular imaging analysis of Rab GTPases in the regulation of phagocytosis and macropinocytosis. *Anat Sci Int* 2016; **91**:35–42.
55. Mi Y, Coonce M, Fiete D, Steirer L, Dveksler G, Townsend RR, Baenziger JU. Functional consequences of mannose and asialoglycoprotein receptor ablation. *J Biol Chem* 2016; **291**:18700–18717.
56. Kang JH, Sim JS, Zheng T, Yim M. F4/80 inhibits osteoclast differentiation via downregulation of nuclear factor of activated T cells, cytoplasmic 1. *Arch Pharm Res* 2017; **40**:492–499.
57. Tsou CL, Peters W, Si Y, Slaymaker S, Aslanian AM, Weisberg SP, Mack M, Charo IF. Critical roles for CCR2 and MCP-3 in monocyte mobilization from bone marrow and recruitment to inflammatory sites. *J Clin Invest* 2007; **117**:902–909.
58. Rosas M, Thomas B, Stacey M, Gordon S, Taylor PR. The myeloid 7/4-antigen defines recently generated inflammatory macrophages and is synonymous with Ly-6B. *J Leukoc Biol* 2010; **88**:169–180.
59. Foey AD, Feldmann M, Brennan FM. CD40 Ligation induces macrophage IL-10 and TNF-α Production: differential use of the PI3K and p42/44 Mapk-Pathways. *Cytokine* 2001; **16**:131–142.
60. Portillo JA, Feliciano LM, Okenka G, Heinzel F, Subauste MC, Subauste CS. CD40 and tumour necrosis factor-a co-operate to up-regulate

inducuble nitric oxide synthase expression in macrophages. *Immunology* 2012; **135**:140–150.
61. Mantovani A, Sica A, Sozzani S, Allavena P, Vecchi A, Locati M. The chemokine system in diverse forms of macrophage activation and polarization. *Trends Immunol* 2004; **25**:677–686.
62. Murray PJ, Wynn TA. Protective and pathogenic functions of macrophage subsets. *Nat Rev Immunol* 2011; **11**:723–737.
63. Couri BM, Lenis AT, Borazjani A, Balog BM, Kuang M, Butler RS, Penn MS, Damaser MS. Effect of pregnancy and delivery on cytokine expression in a mouse model of pelvic organ prolapse. *Female Pelvic Med Reconstr Surg* 2017; **23**:449–456.
64. Mantovani A, Biswas SK, Galdiero MR, Sica A, Locati M. Macrophage plasticity and polarization in tissue repair and remodelling. *J Pathol* 2013; **229**:176–185.
65. Ferrante CJ, Pinhal-Enfield G., Elson G., Cronstein BN, Hasko G, Outram S, Leibovich S. J. The adenosine-dependent angiogenic switch of macrophages to an M2-like phenotype is independent of interleukin-4 receptor alpha (IL-4Rα) signaling. *Inflammation* 2013; **36**:921–931.
66. Davis MJ, Tsang TM, Qiu Y, Dayrit JK, Freij JB, Huffnagle GB, Olszewski MA. Macrophage M1/M2 polarization dynamically adapts to changes in cytokine microenvironments in Cryptococcus neoformans infection. *mBio* 2013; **4**:e00264–13
67. Srikhajon K, Shynlova O, Preechapornprasert A, Chanrachakul B, Lye S. A new role for monocytes in modulating myometrial inflammation during human labor. *Biol Reprod* 2014; **91**:10.
68. Moraes SG, Campos Pinheiro M, Toledo OM, Joazeiro PP. Phenotypic modulation of fibroblastic cells in mice pubic symphysis during pregnancy, partum and postpartum. *Cell Tissue Res* 2004; **315**:223–231.